Received: 30 December 2023 | Revised: 20 February 2024 | Accepted: 5 March 2024

DOI: 10.1002/psp4.13127

ARTICLE

Physiologically based pharmacokinetic modeling of imatinib and *N*-desmethyl imatinib for drug–drug interaction predictions

Helena Leonie Hanae Loer[1] | **Christina Kovar**[1,2] | **Simeon Rüdesheim**[1,2] | **Fatima Zahra Marok**[1] | **Laura Maria Fuhr**[1] | **Dominik Selzer**[1] | **Matthias Schwab**[2,3,4] | **Thorsten Lehr**[1]

[1]Clinical Pharmacy, Saarland University, Saarbrücken, Germany

[2]Dr. Margarete Fischer-Bosch-Institute of Clinical Pharmacology, Stuttgart, Germany

[3]Departments of Clinical Pharmacology, and Pharmacy and Biochemistry, University of Tübingen, Tübingen, Germany

[4]Cluster of Excellence iFIT (EXC2180), Image-Guided and Functionally Instructed Tumor Therapies, University of Tübingen, Tübingen, Germany

Correspondence
Thorsten Lehr, Clinical Pharmacy, Saarland University, Campus C4 3, 66123 Saarbrücken, Germany.
Email: thorsten.lehr@mx.uni-saarland.de

Abstract

The first-generation tyrosine kinase inhibitor imatinib has revolutionized the development of targeted cancer therapy and remains among the frontline treatments, for example, against chronic myeloid leukemia. As a substrate of cytochrome P450 (CYP) 2C8, CYP3A4, and various transporters, imatinib is highly susceptible to drug–drug interactions (DDIs) when co-administered with corresponding perpetrator drugs. Additionally, imatinib and its main metabolite *N*-desmethyl imatinib (NDMI) act as inhibitors of CYP2C8, CYP2D6, and CYP3A4 affecting their own metabolism as well as the exposure of co-medications. This work presents the development of a parent–metabolite whole-body physiologically based pharmacokinetic (PBPK) model for imatinib and NDMI used for the investigation and prediction of different DDI scenarios centered around imatinib as both a victim and perpetrator drug. Model development was performed in PK-Sim® using a total of 60 plasma concentration–time profiles of imatinib and NDMI in healthy subjects and cancer patients. Metabolism of both compounds was integrated via CYP2C8 and CYP3A4, with imatinib additionally transported via P-glycoprotein. The subsequently developed DDI network demonstrated good predictive performance. DDIs involving imatinib and NDMI were simulated with perpetrator drugs rifampicin, ketoconazole, and gemfibrozil as well as victim drugs simvastatin and metoprolol. Overall, 12/12 predicted DDI area under the curve determined between first and last plasma concentration measurements (AUC_{last}) ratios and 12/12 predicted DDI maximum plasma concentration (C_{max}) ratios were within twofold of the respective observed ratios. Potential applications of the final model include model-informed drug development or the support of model-informed precision dosing.

Study Highlights

WHAT IS THE CURRENT KNOWLEDGE ON THE TOPIC?

As a victim drug of cytochrome P450 (CYP) 2C8, CYP3A4, and P-glycoprotein, imatinib is highly susceptible to drug–drug interactions (DDIs). Additionally, acting as a perpetrator, imatinib affects its own metabolism and the exposure of co-medications via inhibition of CYP2C8, CYP2D6, and CYP3A4.

WHAT QUESTION DID THIS STUDY ADDRESS?

This study presents the development of a new whole-body physiologically based pharmacokinetic model of imatinib and its main metabolite *N*-desmethyl imatinib (NDMI). The model was applied to describe and predict the role of imatinib and NDMI as victims and perpetrators within a newly established CYP2C8/CYP2D6/CYP3A4/P-glycoprotein-DDI network.

WHAT DOES THIS STUDY ADD TO OUR KNOWLEDGE?

The DDI network helps to evaluate the effects of co-medication on the pharmacokinetics of imatinib/NDMI and the inhibitory potential of imatinib/NDMI, highlighting the importance of considering imatinib as both victim and perpetrator in clinical practice.

HOW MIGHT THIS CHANGE DRUG DISCOVERY, DEVELOPMENT, AND/OR THERAPEUTICS?

The model can be used to support model-informed drug development and to improve clinical safety and efficacy of imatinib and co-medications through model-based precision dosing.

INTRODUCTION

In 2001, approval of the tyrosine kinase inhibitor (TKI) imatinib for the treatment of Philadelphia chromosome-positive chronic myeloid leukemia (CML) revolutionized not only the therapy of CML, but also the development of targeted cancer therapy in general.[1] Imatinib selectively inhibits the *BCR-ABL* oncoprotein encoded by the Philadelphia chromosome, suppressing its constitutive tyrosine kinase activity and associated uncontrolled proliferation.[2] However, resistance to imatinib, primarily due to mutations in the *BCR-ABL* oncogene and other factors, necessitated the development of subsequent generations of TKIs.[3] Despite this, imatinib remains one of the frontline therapies for CML and has been approved for additional indications, such as acute lymphoblastic leukemia and gastrointestinal stromal tumors (GISTs).[4]

As a Biopharmaceutics Classification System class I drug, imatinib demonstrates high intestinal permeability and solubility.[5] When administered orally, it is completely absorbed, achieving an absolute bioavailability exceeding 97%.[6] Imatinib is primarily metabolized via cytochrome P450 (CYP) enzymes 2C8 and 3A4,[7] with its main metabolite, *N*-desmethyl imatinib (NDMI), accounting for 10%–15% of the overall drug level. NDMI's potency against *BCR-ABL* is approximately three times lower than that of imatinib itself.[8,9] Furthermore, imatinib has been identified as a substrate of numerous influx and efflux transporters in vitro, such as organic cation transporter (OCT) 1, OCTN2, organic-anion-transporting polypeptide (OATP) 1A2, OATP1B3, breast cancer resistance protein (BCRP), and P-glycoprotein (P-gp).[10–12] Following oral administration, 67% and 13% of a single dose (SD) of imatinib are excreted as imatinib-related products in feces and urine, respectively, over a period of 7 days.[13]

Imatinib and its metabolite NDMI are highly susceptible to drug–drug interactions (DDIs), impacting their own metabolism and altering the exposure of co-administered drugs via inhibition of CYP2C8, CYP2D6, and CYP3A4.[14,15] For instance, pretreatment with imatinib resulted in a 2.6-fold increase in the area under the curve (AUC) of the active metabolite of simvastatin, which is formed by CYP3A4.[16] Consequently, the United States Food and Drug Administration (FDA) lists imatinib as a moderate inhibitor of CYP3A4.[17] However, imatinib does not only act as a perpetrator but also as a victim drug in DDI scenarios. Here, perpetrator drugs affecting imatinib's and NDMI's metabolism via CYP2C8 and CYP3A4 are of particular clinical importance. For example, concomitant administration with the antifungal agent ketoconazole, an inhibitor, increases imatinib exposure by 40%. In contrast, pretreatment with the antibiotic agent rifampicin, an inducer, leads to a 74% reduction in AUC of imatinib.[18,19] Given the typical

prescription of five to eight drugs per patient in oncology, these interactions present a substantial challenge in terms of therapeutic management during imatinib treatment. A co-medication review of over 4500 patients receiving imatinib identified potential DDIs associated with a decrease in imatinib effectiveness in 43% and an increase in toxicity in 68% of cases.[20]

Given these complexities, there is a critical need to understand the pharmacokinetics (PK) of imatinib and NDMI, especially regarding their interaction potential. This understanding is vital to enhance the safety and efficacy of imatinib therapy. Therefore, this study aimed to develop a whole-body physiologically based pharmacokinetic (PBPK) model for imatinib and its main metabolite NDMI. Such models are exceptionally useful in investigating the PK of drugs, both independently and within DDI frameworks, as emphasized by the substantial number of PBPK studies submitted to regulatory agencies concentrating on DDI research questions.[21] Furthermore, the versatility of PBPK modeling, especially in integrating patient-specific demographic, physiological, pathophysiological, and pharmacogenetic data, makes it instrumental in facilitating model-based precision dosing strategies.[22] Utilizing the developed imatinib model, this study further conducted predictions and analyses of various complex DDI scenarios, showcasing imatinib as both a victim and perpetrator of such interactions. Numerous PBPK models of imatinib have been developed to explore various research inquiries.[23–25] However, our approach uniquely extends this body of work by providing a comprehensive whole-body PBPK model that incorporates imatinib's main metabolite NDMI, and examines imatinib as both a victim and a perpetrator drug in DDI scenarios. To promote widespread access and encourage further research, the finalized model files will be made available to the public at http://models.clinicalpharmacy.me/.

METHODS

Software

Development of the imatinib PBPK model, including parameter identification and local sensitivity analyses, was performed using PK-Sim® and MoBi® version 11.0 (Open Systems Pharmacology Suite, www.open-systems-pharmacology.org, 2022). Engauge Digitizer version 12.1 (M. Mitchell, https://markummitchell.github.io/engauge-digitizer/, 2019) was utilized for the digitization of published clinical study data according to Wojtyniak et al.[26] The R programming language version 4.2.3 (R Foundation for Statistical Computing, Vienna, Austria, 2023) was used to generate plots and calculate PK parameters as well as quantitative model performance measures.

Clinical study data

Plasma concentration–time profiles of imatinib and its main metabolite NDMI were gathered from published literature covering a wide dosing range of imatinib administered either intravenously or orally in SD and multiple dose (MD) studies. Once digitized, the profiles were systematically divided into a training and a test dataset for model development and model evaluation, respectively. The allocation of profiles was conducted in a deliberate, non-randomized fashion. The goal was to construct a training dataset that encompassed a diverse range of dosages and administration forms, ensuring each profile included a wide array of sampling time points over an extended duration. Concurrently, the approach aimed to optimize the size of the test dataset, thereby enhancing its robustness for thorough model evaluation. Only profiles obtained from healthy individuals were selected for the training dataset, whereas CML and GIST patients were included in the test dataset.

Physiologically based pharmacokinetic model building

Prior to building the imatinib parent–metabolite model, an extensive literature search was conducted regarding clinical study data and physicochemical parameters as well as information on the absorption, distribution, metabolism, and excretion (ADME) of imatinib and NDMI.

For model simulations, a representative virtual individual was created for each included study population based on the corresponding reported mean and mode data for age, sex, weight, height, body mass index, and ethnicity. If demographic information was missing or incomplete, a default individual was generated according to the population database provided in PK-Sim®. Relative expressions of relevant transporters and enzymes in the different organs were adopted from the expression database included in PK-Sim®. Tables S1 and S2 list the reference concentration in the respective organ of highest concentration as well as the relative expression profile for each implemented transporter/enzyme. To visually examine the influence of variation in demographic factors, plasma protein binding to α1-acid glycoprotein (AGP), as well as transporter and metabolizing enzyme abundances on the exposure of imatinib and NDMI, a virtual population of 1000 individuals was established for each study population. If no minimum

and maximum demographic values were provided, an age range of 20–50 years was assumed. Geometric standard deviations applied to the incorporated transporter/enzyme concentrations for the population sampling process are presented in Table S1.

During the parameter identification process, unknown parameter values not reported in the literature or parameters involved in PK-Sim®'s permeability and partition quantitative structure–activity relationship (QSAR) models were fitted using the training dataset. Following oral administration, the release of imatinib was incorporated via a Weibull function (Equation S1). Depending on the information available in the literature, transport and metabolic processes were implemented as either Michaelis–Menten (MM) (Equation S2) or first-order kinetics. The role of relevant enzymes in imatinib metabolism was informed by including published in vitro data, detailing the proportional contribution of each relevant enzyme to the total clearance of imatinib, thereby informing the PBPK model with more precise metabolic pathway information.

Physiologically based pharmacokinetic model evaluation

The imatinib parent–metabolite model was evaluated both graphically and statistically. First, predicted plasma concentration–time profiles of imatinib and NDMI were plotted alongside corresponding observed data. Goodness-of-fit plots were generated to assess the deviation of predicted versus observed plasma concentrations, AUC determined between first and last plasma concentration measurements (AUC_{last}), and maximum plasma concentration (C_{max}) values for each profile. A twofold difference from observed values was set as the prediction success threshold. The statistical analysis covered the calculation of mean relative deviations (MRDs) for predicted concentration–time points (Equation 1) and geometric mean fold errors for predicted AUC_{last} and C_{max} values (Equation 2).

$$\mathrm{MRD} = 10^{x}; x = \sqrt{\frac{\sum_{i=1}^{k} \left(\log_{10}\hat{c}_i - \log_{10}c_i\right)^2}{k}} \quad (1)$$

where c_i = i-th observed concentration, $\hat{c}_i$ = predicted concentration corresponding to the i-th observed concentration, and k = number of observed values.

$$\mathrm{GMFE} = 10^{x}; x = \frac{\sum_{i=1}^{m} \left|\log_{10}\left(\frac{\hat{p}_i}{p_i}\right)\right|}{m} \quad (2)$$

where p_i = observed AUC_{last} or C_{max} value of study i, $\hat{p}_i$ = corresponding predicted AUC_{last} or C_{max} value of study i, and m = number of studies.

Finally, local sensitivity analyses were conducted for imatinib and NDMI, which are described in Section S2.7.1.

Drug–drug interaction network modeling

To investigate the role of imatinib and NDMI acting as either victims or perpetrators in DDI scenarios, the developed model was coupled with previously published PBPK models of rifampicin, ketoconazole, gemfibrozil, simvastatin, and metoprolol.[27–31] Relevant interaction types, including induction, competitive inhibition, noncompetitive inhibition, and mechanism-based inactivation, were incorporated as described in the Open Systems Pharmacology Suite manual,[32] with the corresponding interaction parameters adopted from the literature.

The developed DDI network was graphically evaluated by comparing predicted with observed plasma concentration–time profiles of each victim drug with and without co-administration of the respective perpetrator drug. Predicted and observed AUC_{last} and C_{max} ratios were calculated for each DDI scenario according to Equation 3 and compared by applying the limits proposed by Guest et al.[33] to determine prediction accuracy (including 20% variability).

$$\text{DDI PK parameter ratio} = \frac{\text{PK parameter}_{\mathrm{DDI}}}{\text{PK parameter}_{\mathrm{Control}}} \quad (3)$$

where PK parameter = AUC_{last} or C_{max}, PK parameter$_{DDI}$ = AUC_{last} or C_{max} of victim drug with perpetrator co-administration, and PK parameter$_{Control}$ = AUC_{last} or C_{max} of victim drug control.

Quantitative evaluation was performed by calculating GMFE values (Equation 2) for all predicted DDI AUC_{last} and C_{max} ratios.

RESULTS

Physiologically based pharmacokinetic model building and evaluation

The imatinib parent–metabolite model was developed using 24 clinical studies providing a total of 42 and 18 plasma concentration–time profiles of imatinib and NDMI, respectively. The profiles were allocated to either the training (n = 8) or the test (n = 52) dataset. Of these 60 profiles, 40 were collected in healthy subjects, while 20 were derived from CML and GIST patients. Given no apparent difference between plasma profiles of healthy subjects and patients, the developed PBPK model was applied to CML and GIST patients without modifications

to the drug-dependent parameters of imatinib and NDMI or the physiological parameters of the simulated virtual individuals. Routes of administration included intravenous dosing of imatinib via infusion (100 mg, SD) and oral intake as tablet or capsule (25–750 mg, SD and MD). Information on all profiles and study populations used is listed in Table S3.

Figure 1 provides a schematic representation of the transport and metabolic processes implemented in the model. Imatinib metabolism via CYP2C8 and CYP3A4 was incorporated in the model via MM kinetics, accounting for 67% and 33% of NDMI formation, respectively. The model further integrated the transformation of imatinib into unspecified metabolites through CYP3A4, following first-order kinetics. Additionally, P-gp was incorporated as a transport protein for imatinib, with its function modeled using MM kinetics. NDMI metabolism was implemented via CYP2C8, CYP3A4, and a nonspecific first–order hepatic clearance process. The effect of genetic polymorphisms on the incorporated transporters and enzymes was not accounted for in the model due to a lack of studies stratifying their cohorts by genotype or phenotype.

During model building, lipophilicities of imatinib and NDMI which are crucial parameters in several key QSAR equations were optimized. This fitting resulted in values within the reference range for imatinib and approximately one logarithmic unit lower than the reference for NDMI.

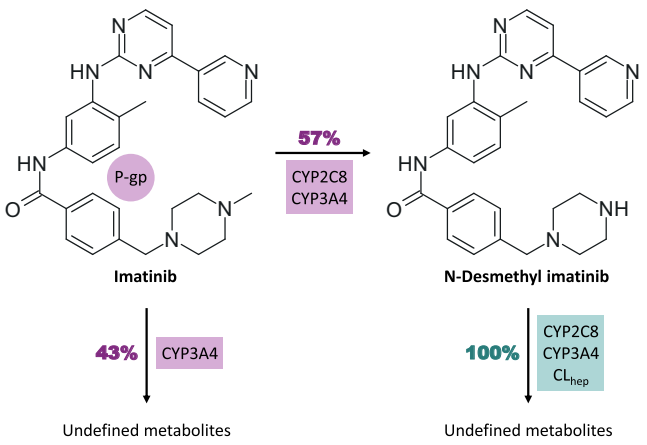

FIGURE 1 Schematic overview of the processes incorporated in the developed imatinib parent–metabolite model. Following administration of a single dose of imatinib, 57% of modeled imatinib metabolism leads to the formation of *N*-desmethyl imatinib via CYP2C8 and CYP3A4, while the remaining pathway involves the conversion of imatinib to undefined metabolites via CYP3A4. In addition, transport via P-gp was included for imatinib. For the metabolism of *N*-desmethyl imatinib, the model incorporates CYP2C8, CYP3A4, and a nonspecific hepatic clearance process. CL_{hep}: hepatic clearance, CYP: cytochrome P450, P-gp: P-glycoprotein.

Parameters for first–order clearance processes were also included in the parameter optimization procedure. For biotransformation steps modeled as MM kinetics, MM constants (K_M) were adopted from the literature, while catalytic rate constants (k_{cat}) were fitted within one magnitude of reported values. Conversely, both K_M and k_{cat} were optimized for the transport of imatinib via P-gp, as the K_M value could not be informed from the literature. In addition, (auto)inhibition was integrated using published data.[14,34,35] Here, for imatinib, mechanism-based inactivation of CYP3A4 was implemented. Moreover, competitive inhibition of CY2C8, CYP2D6, P-gp, and BCRP was integrated. With respect to NDMI, competitive inhibition parameters of CYP2C8, CYP2D6, and CYP3A4 were informed via literature.[14] A Weibull function was applied to simulate the release of imatinib from both tablets and capsules, with parameters time to 50% dissolution and shape derived from a tablet dissolution profile of previous work according to Langenbucher et al.[36,37] The final model parameters for imatinib and NDMI are provided in Table S4.

The developed imatinib PBPK model demonstrated good performance in describing (training dataset) and predicting (test dataset) plasma concentration–time profiles of imatinib and NDMI following intravenous and oral administration of imatinib to healthy subjects and patients. Figure 2 presents a representative selection of imatinib/NDMI population predictions compared to corresponding observed data. Linear and semilogarithmic plots of all model predictions including observed data are provided in Sections S2.1–S2.3.

Goodness-of-fit plots of predicted versus observed plasma concentrations as well as AUC_{last} and C_{max} values separated by dataset are shown in Figure 3. Overall, 92% of predicted imatinib and NDMI concentration measurements as well as 98% of predicted AUC_{last} and 98% of predicted C_{max} values were within twofold of corresponding observed data. Moreover, statistical model evaluation resulted in a mean (range) MRD of predicted plasma concentrations of 1.46 (1.07–2.81) along with mean (range) $GMFE_{AUClast}$ and $GMFEC_{max}$ values of 1.28 (1.00–2.40) and 1.26 (1.00–2.08), respectively. Values for MRD, AUC_{last}, and C_{max} of all profiles are listed in Tables S5 and S6.

Local sensitivity analyses were performed based on simulated steady-state conditions following oral administration of 400 mg imatinib once daily for 28 days. The steady-state AUC of imatinib and NDMI exhibited the greatest sensitivity to changes in the acid dissociation constant of the amino group within the piperazine ring and the unbound fraction (f_u), respectively. Both parameters were adopted from the literature. Of note, given the proximity of the model parameter for the acid dissociation constant (7.84) to the physiological pH of 7.4, an increase of 10% causes only a small change in imatinib and NDMI

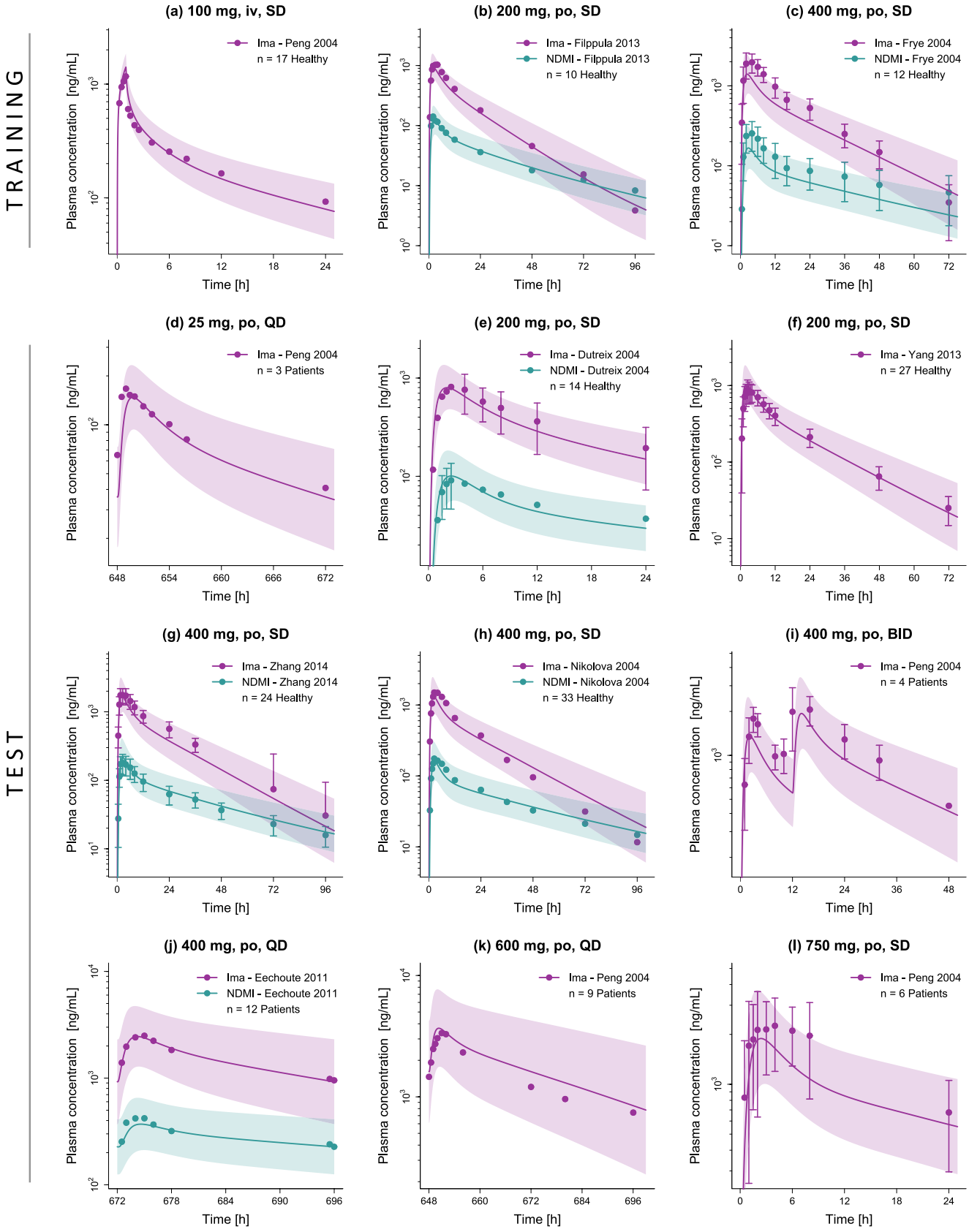

FIGURE 2 Predicted compared to observed plasma concentration–time profiles of imatinib and NDMI of the training (a–c) and test (d–l) dataset. Solid lines and ribbons represent population predictions ($n = 1000$; geometric mean and geometric standard deviation), while corresponding observed data are shown as dots (± standard deviation, if available).[6,18,38,43,47–51] Detailed information on all investigated profiles is provided in Table S3. BID: twice daily, Healthy: healthy subjects, Ima: imatinib, iv: intravenous, *n*: number of study participants, NDMI: *N*-desmethyl imatinib, Patients: cancer patients, po: oral, QD: once daily, SD: single dose.

AUC values, while a reduction of 10% is associated with a large decrease in exposure. Section S2.7.2 provides a detailed evaluation of the sensitivity analyses.

Drug–drug interaction modeling

The DDI network centered around imatinib as a victim and perpetrator drug was developed using five DDI studies. In total, three studies investigated the influence of perpetrator co-administration on the exposure of imatinib and NDMI. Here, one study examined pretreatment with the competitive CYP2C8/CYP3A4/P-gp inhibitor and inducer rifampicin, while a second study addressed co-treatment with the competitive CYP3A4/P-gp inhibitor and non-competitive CYP2C8 inhibitor ketoconazole.[18,19] Finally, one study analyzed the effect of pretreatment with the CYP2C8 mechanism-based inactivator gemfibrozil.[38]

Moreover, DDI studies assessing the influence of imatinib pretreatment on the PK of simvastatin and metoprolol as well as their active metabolites were available, with interactions predominantly caused by CYP3A4 mechanism-based inactivation and CYP2D6 competitive inhibition, respectively.[15,16] In the case of metoprolol, a drug–drug–gene interaction (DDGI) study was included in which the study population was additionally stratified into CYP2D6 normal metabolizers (NMs) and intermediate metabolizers (IMs). Here, the same K_M value was used for both study cohorts, while phenotype-specific k_{cat} values were applied.[28] Because most NMs and IMs were **1/*10* and **10/*10* genotypes, respectively, k_{cat} values equivalent to 64% and 19% of the wildtype k_{cat} were included in the DDI model. Figure 4 shows a schematic overview of the modeled DDI network, depicting the respective main interaction mechanisms. Detailed information on the DDI studies used and model parameters of each DDI partner are available in Sections S3.1–S3.2.

Predicted versus observed plasma concentration–time profiles of each victim drug with and without co-administration of the respective perpetrator drug are displayed in Figure 5. Table 1 presents the predicted versus observed impact of each perpetrator on the respective victim, stating the exposure (AUC) during perpetrator co-administration relative to the control exposure. Furthermore, predicted versus observed DDI AUC_{last} and C_{max} ratios are shown in Figure 6. In total, 11/12 of predicted DDI AUC_{last} and 10/12 of C_{max} ratios were within the limits proposed by Guest et al.[33] with mean (range) GMFE values of 1.21 (1.02–1.65) and 1.23 (1.01–1.87), respectively. Predicted and observed DDI profiles (linear and semilogarithmic) and corresponding DDI ratios are provided in Sections S3.3–S3.6.

DISCUSSION

In the present work, a parent–metabolite whole-body PBPK model for imatinib was developed demonstrating its capability to accurately describe and predict plasma concentration–time profiles for both imatinib and its main metabolite NDMI. The model is robust across a wide dosing range of intravenously and orally administered imatinib (25–750 mg, SD and MD studies) in both healthy subjects and cancer patients. PK differences between these populations are documented in the literature and were investigated during model building. For instance, a 2–5-fold increase in AGP plasma levels is reported for CML patients compared to healthy subjects, potentially influencing imatinib f_u.[39] However, since elevated AGP levels were also observed to normalize during imatinib treatment, no CML-specific f_u value was incorporated in the model.[40] Overall, imatinib clearance in CML patients appears to depend on both the disease stage and the duration of imatinib use, while in GIST patients, for example, changes in liver function due to hepatic metastases or surgery have been reported.[40] Given the frequent unavailability of detailed physiological data for cancer patients, mechanistic modeling to account for these differences was constrained. Therefore, our approach remained focused on leveraging broadly applicable physiological parameters. Moreover, given the performance of the unmodified model in both populations (mean MRD: healthy subjects 1.39 vs. patients 1.59), no population-specific adjustments were made to minimize the model's complexity. The final PBPK model was further applied to predict different DDI scenarios involving imatinib and NDMI acting as both victims and perpetrators.

A key constraint of the model lies in the limitations of current knowledge as well as published clinical and in vitro data. For instance, consistent with literature data, when simulating an oral administration of 400 mg imatinib, the entire dose is absorbed.[6] However, at 83%, the predicted total bioavailability was moderately lower than the reported literature value of more than 97%.[6] One potential explanation for this discrepancy may lie in the in vivo deconjugation of imatinib glucuronides by gut microbes,[41] a process integral to the enterohepatic circulation (EHC). This phenomenon could lead to the reabsorption of imatinib, influencing its overall bioavailability. Although the model accounts for the EHC of imatinib with a modeled EHC fraction of 1, it does not incorporate the sequential formation and breakdown of imatinib glucuronides. This omission is primarily due to the complexity of these processes and the lack of comprehensive data regarding the conjugation and deconjugation of imatinib, as well as the PK of its various glucuronide forms.

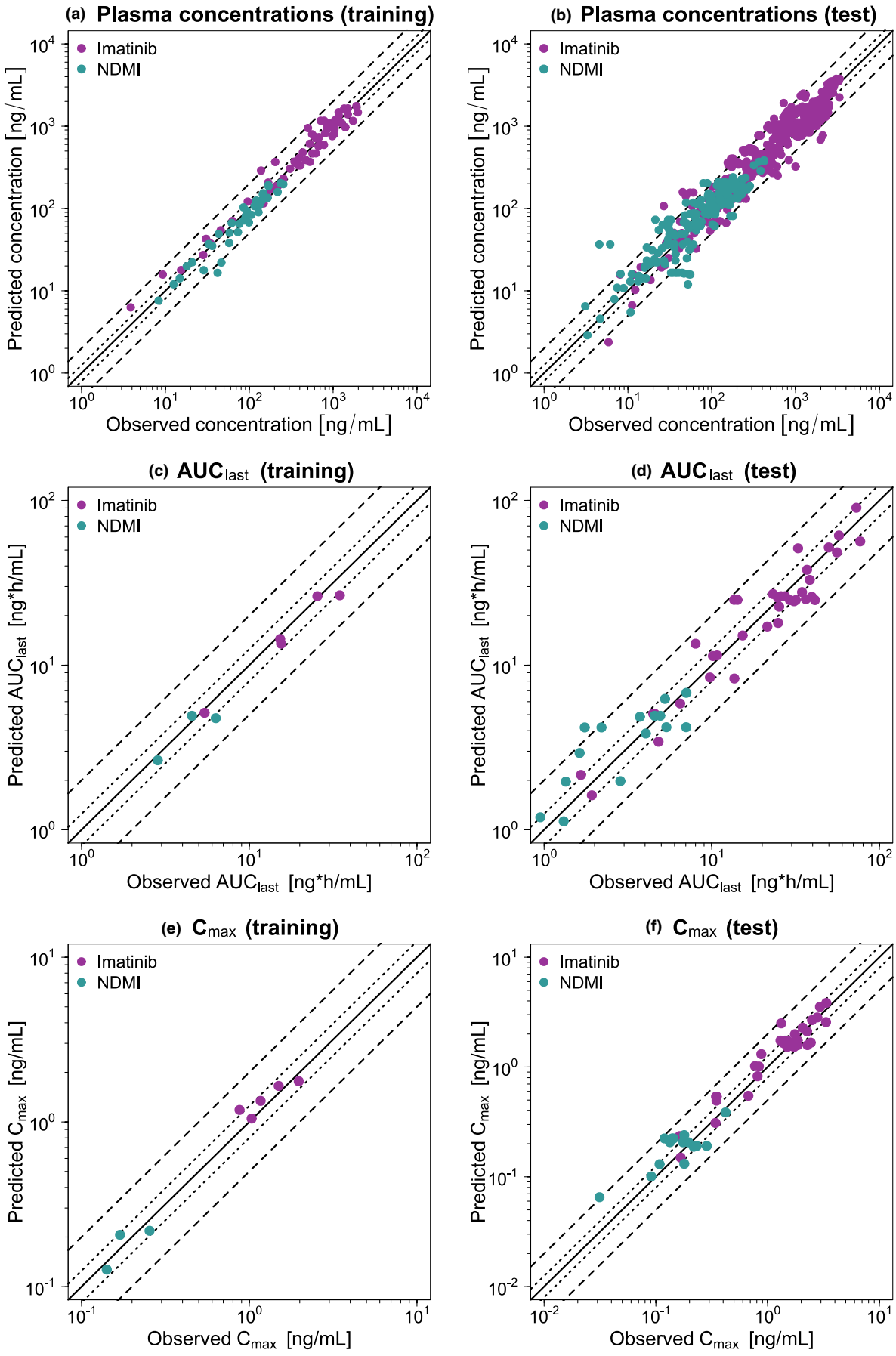

FIGURE 3 Goodness-of-fit plots of the final imatinib parent–metabolite model. Stratified by training (left column) and test dataset (right column), predicted plasma concentration measurements (a, b) as well as AUC_{last} (c, d) and C_{max} (e, f) values are plotted against corresponding observed data. The solid line represents the line of identity, while dotted lines indicate 1.25-fold, and dashed lines twofold deviation from the respective observed value. Detailed information on all investigated profiles is provided in Table S3. AUC_{last}: area under the curve determined between first and last plasma concentration measurements, C_{max}: maximum plasma concentration, NDMI: *N*-desmethyl imatinib.

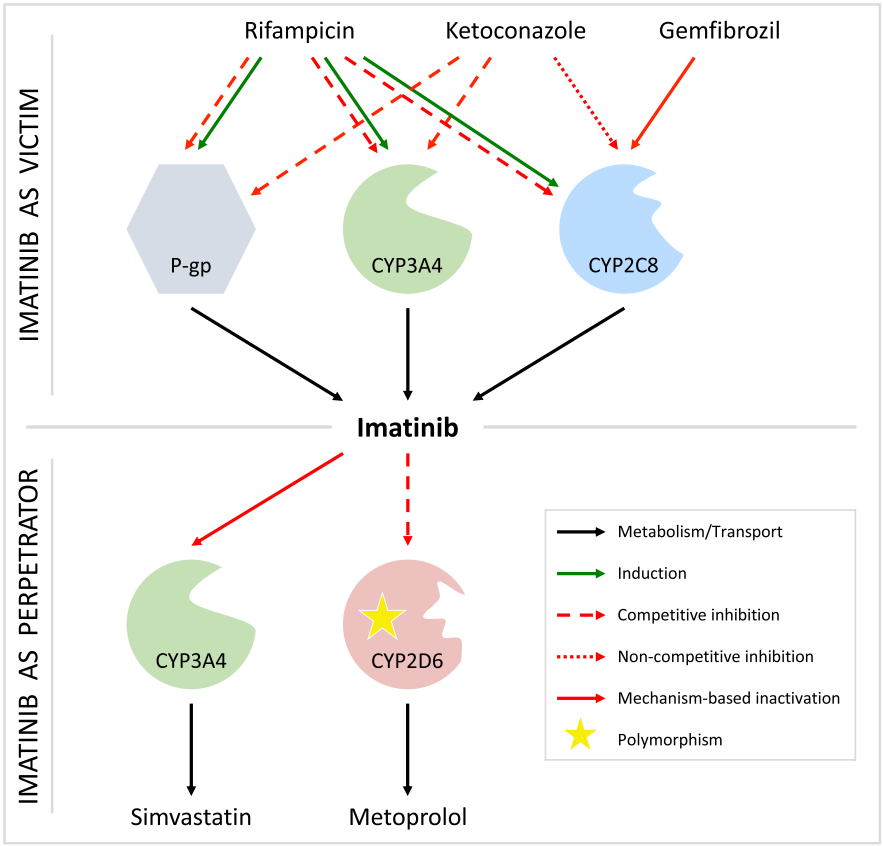

FIGURE 4 Schematic overview of the modeled drug–drug interaction network. The network covers the effects of rifampicin, ketoconazole, and gemfibrozil on the pharmacokinetics of imatinib as a victim, as well as the impact of imatinib as a perpetrator on the plasma levels of simvastatin and metoprolol. The respective main mechanisms of interactions are presented. For simplicity, the interaction effects of and on the corresponding metabolites, such as *N*-desmethyl imatinib, are summarized under the name of the parent drug. CYP: cytochrome P450, P-gp: P-glycoprotein.

Furthermore, imatinib has been identified as a substrate of several influx and efflux transporters in vitro, such as OCT1, OCTN2, OATP1A2, OATP1B3, BCRP, and P-gp,[10–12] potentially influencing ADME processes. However, the relevance of these transporters in vivo remains uncertain due to conflicting study results. In our model, P-gp was selected as the efflux transporter over BCRP, primarily because the data for P-gp were more consistent and reliable compared to that for BCRP. Incorporating P-gp into the model led to an increase in the predicted urinary excretion of unchanged imatinib, rising from under 2% to about 5% following SD oral administration. This adjustment brings the model's predictions more in line with the urinary excretion rates observed in vivo.[37,42] During model building, the incorporation of various influx transporters such as OCT1, OCTN2, OATP1A2, and OATP1B3 was tested. Despite considering the integration of these transporters into the model, we ultimately did not include them in the final model. This decision was based on the observation that their inclusion did not markedly alter the base model's predictive performance or the simulated DDIs, with the total bioavailability consistently estimated around 83%. Furthermore, the data on transport parameters necessary to inform the model were limited and often conflicting. For example, while some studies identified OATP1A2 as a key transporter in imatinib uptake, evidence from pretreatment with the OATP1A2 inhibitor rosuvastatin indicated no significant impact on imatinib's PK, adding to the ambiguity in these transporters' roles.[43,44]

Overall, as only one mean intravenous imatinib profile was available from the literature, additional intravenous studies would be of particular interest to further investigate the discrepancy between modeled and reported total bioavailability. Moreover, dedicated studies on the parameterization and quantification of transport processes would be of great value to allow for an even more precise simulation of imatinib's PK. However, as both oral and intravenous administration of imatinib and metabolism to

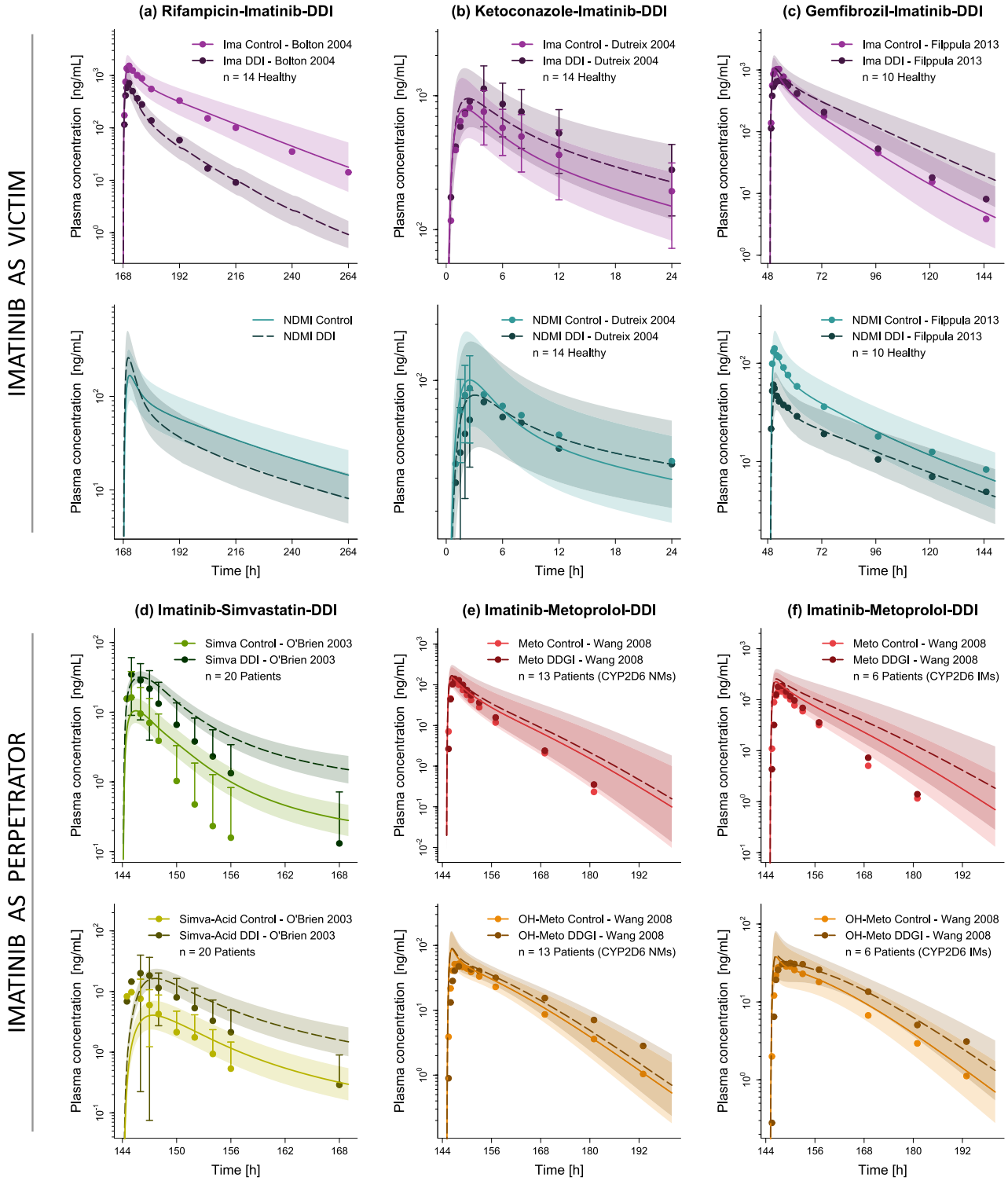

FIGURE 5 Evaluation of the modeled drug–drug interaction network. Presented are predicted plasma concentration–time profiles of victim drugs imatinib (a–c), simvastatin (d), and metoprolol (e, f) without (Control) and with (DDI) co-administration of the respective perpetrator drug rifampicin (a), ketoconazole (b), gemfibrozil (c), or imatinib (d–f), alongside corresponding observed data.[15,16,18,19,38] Solid (Control) and dashed (DDI) lines and ribbons represent model population predictions ($n = 1000$; geometric mean and geometric standard deviation), while corresponding observed data are shown as dots (± standard deviation, if available). For the effect of rifampicin on NDMI, only DDI ratios were reported in the respective study (see Figure 6). Detailed information on all investigated DDI studies is provided in Table S8. CYP: cytochrome P450, DDI: drug–drug interaction, Healthy: healthy subjects, IM: intermediate metabolizer, Ima: imatinib, Meto: metoprolol, *n*: number of study participants, NDMI: *N*-desmethyl imatinib, NM: normal metabolizer, OH-Meto: hydroxymetoprolol, Patients: cancer patients, Simva: simvastatin, Simva-Acid: simvastatin hydroxy acid.

TABLE 1 Predicted versus observed impact on the exposure of each victim drug upon perpetrator co-administration.

Victim	Perpetrator	Compound measured	DDI exposure[a] [%]		References
			Predicted	Observed	
Imatinib	Rifampicin	Imatinib	24	26	Bolton 2004[19]
		NDMI	76	89	
Imatinib	Ketoconazole	Imatinib	144	140	Dutreix 2004[18]
		NDMI	104	86	
Imatinib	Gemfibrozil	Imatinib	151	93	Filppula 2013[38]
		NDMI	54	51	
Simvastatin	Imatinib	Simvastatin	391	322	O'Brien 2003[16]
		Simva-Acid	491	299	
Metoprolol[b]	Imatinib	Metoprolol	119	126	Wang 2008[15]
		OH-Meto	112	129	
Metoprolol[c]	Imatinib	Metoprolol	138	117	Wang 2008[15]
		OH-Meto	133	142	

[a]Relative to the corresponding exposure without perpetrator co-administration.

[b]CYP2D6 normal metabolizers.

[c]CYP2D6 intermediate metabolizers, CYP: cytochrome P450, DDI: drug–drug interaction, NDMI: *N*-desmethyl imatinib, OH-Meto: hydroxymetoprolol, Simva-Acid: simvastatin hydroxy acid.

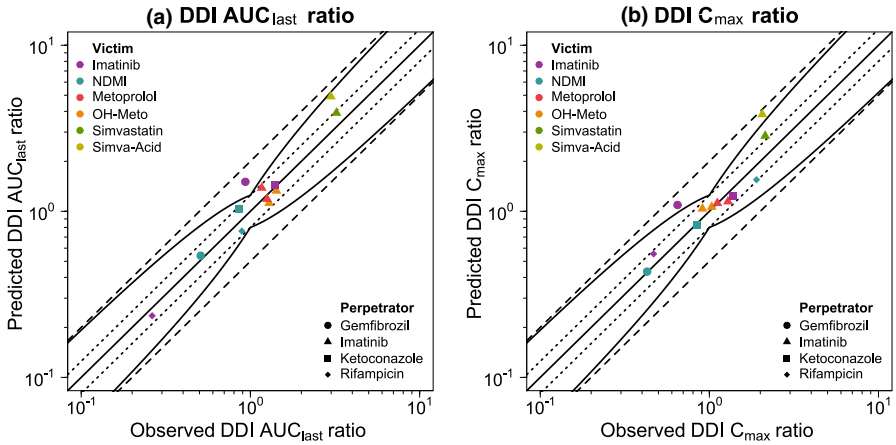

FIGURE 6 Evaluation of the modeled drug–drug interaction network. Predicted versus observed DDI AUC_{last} (a) and DDI C_{max} (b) ratios are shown with the solid line representing the line of identity, dotted lines indicating 1.25-fold, and dashed lines twofold deviation from the respective observed value. Curved lines mark the prediction success limits proposed by Guest et al.[33] including 20% variability. Detailed information on all investigated DDI studies is provided in Table S8. AUC_{last}: area under the curve determined between first and last plasma concentration measurements, C_{max}: maximum plasma concentration, DDI: drug–drug interaction, NDMI: *N*-desmethyl imatinib, OH-Meto: hydroxymetoprolol, Simva-Acid: simvastatin hydroxy acid.

NDMI were well described by the model, we consider hepatic clearance processes, and thus the fraction escaping first-pass liver metabolism, to be adequately represented in the model. Furthermore, the good prediction of mainly metabolic DDIs indicates a well-described relationship between fraction absorbed and fraction escaping gut wall metabolism.

In line with literature reports, CYP2C8 and CYP3A4 were implemented for the metabolism of imatinib and NDMI, while biotransformation via CYP3A5 was excluded due to its relatively minor role in the biotransformation process.[7] Here, model predictions for the relative influence on NDMI formation of CYP2C8 (67%) and CYP3A4 (33%) are in close agreement with the approximate in vitro literature values of 69% and 31%, respectively.[7] Overall, 57% of the modeled total metabolism of imatinib is accounted for by the formation of NDMI, closely aligning with in vitro findings which reported a similar contribution of 51%.[7] Listed fractional contributions of CYP2C8 and CYP3A4 to the metabolism of imatinib refer to a simulated SD

administration of imatinib. However, a shift in the enzymatic contributions toward a greater influence of CYP2C8 was observed upon simulated MD administrations of imatinib, most likely due to the pronounced autoinhibition of CYP3A4. Under simulated steady-state conditions, 75% of imatinib metabolism leads to the formation of NDMI (SD: 57%), with an increasing role of CYP2C8 within the NDMI pathway (SD: 67% vs. MD: 84%). This modeled decrease in CYP3A4 contribution to the overall metabolism of imatinib at steady-state reflects the results from DDI studies involving CYP3A perpetrators. Here an effect of ketoconazole on SD administration of imatinib was observed, while ritonavir showed almost no influence on the steady-state AUC of imatinib.[18,45] This finding could be confirmed via modeling (see Section S3.7). The influence of different polymorphically expressed transporters and enzymes on imatinib exposure has been investigated in previous works. For example, one study showed that the *CYP3A4 rs2242480* polymorphism resulted in significantly lower steady-state imatinib trough concentrations, relative to the wild type.[46] However, the model does not account for genotype-specific activities of the incorporated transporters and enzymes, primarily due to the scarcity of comprehensive data. Future studies focusing on the impact of various genetic polymorphisms on the plasma levels of imatinib and NDMI, especially over extended periods and not just at trough concentrations, would be valuable. Such research could facilitate the integration of, for example, different CYP3A4 activities into the model, allowing more personalized predictions.

Following the model development process, a DDI network centered around imatinib acting as both a victim and perpetrator drug was successfully established by coupling the final imatinib model with previously published models of the perpetrator drugs rifampicin, ketoconazole, and gemfibrozil, as well as of the victim drugs simvastatin and metoprolol.[27–31] Good overall predictive performance was attained for the modeled DDI scenarios, reflected by 24/24 predicted AUC_{last} and C_{max} ratios being within twofold of observed ratios. However, the modeled DDI network has limitations due to incomplete or biased published data. For instance, the effect of co-treatment with ketoconazole on imatinib exposure was examined solely in the context of SD administration of ketoconazole. As the metabolites of ketoconazole also exhibit potent inhibition of CYP2C8, CYP3A4, and P-gp, DDI studies involving pretreatment with ketoconazole would be of great interest to analyze the maximum inhibitory effect of ketoconazole and its metabolites on the AUC of imatinib and NDMI.

Various other PBPK models for imatinib are documented in the literature. These models address aspects such as interethnic differences in imatinib PK as well as dose optimizations for children and adults in DDI scenarios with imatinib as the victim drug.[23–25] Contrasting with these, our whole-body PBPK model of imatinib encompasses the formation and biotransformation of both imatinib and its main metabolite NDMI. This approach is crucial as NDMI not only contributes to imatinib's pharmacodynamic effects but also plays an important role in inhibiting enzymes such as CYP2C8, CYP2D6, and CYP3A4. Hence, the inclusion of NDMI in the model enhances the model's clinical relevance for imatinib application and provides a more robust framework for the prediction of DDIs. While the activity and the inhibitory effect of NDMI are not overly prominent when imatinib is administered alone given its rather low contribution to the overall exposure, the importance of NDMI can increase greatly depending on the concomitant medication. For example, pretreatment with the inducer rifampicin causes the contribution of NDMI to total exposure to increase from 15% to 38%.[19] In a clinical oncology environment with five to eight drugs prescribed per patient, the importance of NDMI might therefore increase considerably and should not be neglected.[20] Furthermore, to the best of our knowledge, the developed DDI network is the first to cover imatinib not only as a victim, but also as a perpetrator drug. In particular, the good model prediction regarding the effect of imatinib on simvastatin exposure, mainly via CYP3A4 inhibition, is of great value as it allows the verification of the appropriate implementation of imatinib autoinhibition.

In summary, the developed imatinib parent–metabolite whole-body PBPK model shows good descriptive and predictive performance for both imatinib and its active metabolite NDMI in healthy subjects and CML/GIST patients. In addition, the role of imatinib and NDMI as CYP2C8, CYP3A4, and P-gp (imatinib) substrates, as well as inhibitors of CYP3A4 and CYP2D6, was successfully investigated and predicted within a newly established DDI network. Potential application areas of the developed model and corresponding imatinib DDI network include model-informed drug development as well as model-based precision dosing for patients. After being evaluated across various DDI scenarios, the imatinib model is capable of integration with any existing and validated PK-Sim® victim or perpetrator model to predict clinically untested DDIs and even multiple DDIs involving more than two DDI partners (e.g., two perpetrators). Hence, the developed imatinib model enables the prediction of effects both by and on imatinib and NDMI across a wide array of clinically relevant polypharmacy scenarios. This capability facilitates the identification and quantification of potential drug interactions. Subsequently, the presented model may be used to generate dose recommendations for imatinib or

relevant victim drugs to improve both therapy safety and efficacy.

AUTHOR CONTRIBUTIONS

H.L.H.L., C.K., D.S., M.S., and T.L. wrote the manuscript. H.L.H.L., C.K., S.R., F.Z.M., L.M.F, and T.L. designed the research. H.L.H.L. performed the research. H.L.H.L. and C.K. analyzed the data.

ACKNOWLEDGMENTS

Open Access funding enabled and organized by Projekt DEAL.

FUNDING INFORMATION

Matthias Schwab was supported by the Robert Bosch Stiftung (Stuttgart, Germany), a grant from the German Federal Ministry of Education and Research (BMBF, 031L0188D, "GUIDE-IBD") and the DFG im Rahmen der Exzellenzstrategie des Bundes und der Länder-EXC 2180-390900677. Thorsten Lehr was supported by the German Federal Ministry of Education and Research (BMBF, Horizon 2020 INSPIRATION grant 643271), under the frame of ERACoSysMed and the European Union Horizon 2021 SafePolyMed (grant 101057639).

CONFLICT OF INTEREST STATEMENT

The authors declared no competing interests for this work.

ORCID

Simeon Rüdesheim https://orcid.org/0000-0002-5741-2511
Matthias Schwab https://orcid.org/0000-0002-9984-075X
Thorsten Lehr https://orcid.org/0000-0002-8372-1465

REFERENCES

1. Kantarjian HM, Jain N, Garcia-Manero G, et al. The cure of leukemia through the optimist's prism. *Cancer*. 2022;128:240-259. doi:10.1002/cncr.33933
2. Kantarjian HM, Talpaz M, Giles F, Brien SO, Cortes J. New insights into the pathophysiology of chronic myeloid leukemia and imatinib resistance. *Ann Intern Med*. 2006;145:913-923. doi:10.7326/0003-4819-145-12-200612190-00008
3. Bixby D, Talpaz M. Seeking the causes and solutions to imatinib-resistance in chronic myeloid leukemia. *Leukemia*. 2011;25:7-22. doi:10.1038/leu.2010.238
4. Roskoski RJ. Properties of FDA-approved small molecule protein kinase inhibitors: a 2023 update. *Pharmacol Res*. 2023;187:106552. doi:10.1016/j.phrs.2022.106552
5. O'Brien Z, Moghaddam MF. A systematic analysis of physicochemical and ADME properties of all small molecule kinase inhibitors approved by US FDA from January 2001 to October 2015. *Curr Med Chem*. 2017;24:3159-3184. doi:10.2174/0929867324666170523124441
6. Peng B, Dutreix C, Mehring G, et al. Absolute bioavailability of imatinib (Glivec®) orally versus intravenous infusion. *J Clin Pharmacol*. 2004;44:158-162. doi:10.1177/0091270003262101
7. Filppula AM, Neuvonen M, Laitila J, Neuvonen PJ, Backman JT. Autoinhibition of CYP3A4 leads to important role of CYP2C8 in imatinib metabolism: variability in CYP2C8 activity may alter plasma concentrations and response. *Drug Metab Dispos*. 2013;41:50-59. doi:10.1124/dmd.112.048017
8. Duckett DR, Cameron MD. Metabolism considerations for kinase inhibitors in cancer treatment. *Expert Opin Drug Metab Toxicol*. 2010;6:1175-1193. doi:10.1517/17425255.2010.506873. Metabolism
9. Manley PW. Investigations into the potential role of metabolites on the anti-leukemic activity of imatinib, nilotinib and midostaurin. *Chimia*. 2019;73:561-570. doi:10.2533/chimia.2019.561
10. Hu S, Franke RM, Filipski KK, et al. Interaction of imatinib with human organic ion carriers. *Clin Cancer Res*. 2008;14:3141-3148. doi:10.1158/1078-0432.CCR-07-4913
11. Hamada A, Miyano H, Watanabe H, Saito H. Interaction of imatinib mesilate with human P-glycoprotein. *J Pharmacol Exp Ther*. 2003;307:824-828. doi:10.1124/jpet.103.055574
12. Burger H, van Tol H, Boersma AWM, et al. Imatinib mesylate (STI571) is a substrate for the breast cancer resistance protein (BCRP)/ABCG2 drug pump. *Blood*. 2004;104:2940-2942. doi:10.1182/blood-2004-04-1398
13. Gschwind HP, Pfaar U, Waldmeier F, et al. Metabolism and disposition of imatinib mesylate in healthy volunteers. *Drug Metab Dispos*. 2005;33:1503-1512. doi:10.1124/dmd.105.004283
14. Filppula AM, Laitila J, Neuvonen PJ, Backman JT. Potent mechanism-based inhibition of CYP3A4 by imatinib explains its liability to interact with CYP3A4 substrates. *Br J Pharmacol*. 2012;165:2787-2798. doi:10.1111/j.1476-5381.2011.01732.x
15. Wang Y, Zhou L, Dutreix C, et al. Effects of imatinib (Glivec) on the pharmacokinetics of metoprolol, a CYP2D6 substrate, in Chinese patients with chronic myelogenous leukaemia. *Br J Clin Pharmacol*. 2008;65:885-892. doi:10.1111/j.1365-2125.2008.03150.x
16. O'Brien SG, Meinhardt P, Bond E, et al. Effects of imatinib mesylate (ST1571, Glivec) on the pharmacokinetics of simvastatin, a cytochrome P450 3A4 substrate, in patients with chronic myeloid leukaemia. *Br J Cancer*. 2003;89:1855-1859. doi:10.1038/sj.bjc.6601152
17. Drug development and drug interactions: FDA table of substrates, inhibitors and inducers. Accessed September 28, 2023. https://www.fda.gov/drugs/drug-interactions-labeling/healthcare-professionals-fdas-examples-drugs-interact-cyp-enzymes-and-transporter-systems
18. Dutreix C, Peng B, Mehring G, et al. Pharmacokinetic interaction between ketoconazole and imatinib mesylate (Glivec) in healthy subjects. *Cancer Chemother Pharmacol*. 2004;54:290-294. doi:10.1007/s00280-004-0832-z
19. Bolton AE, Peng B, Hubert M, et al. Effect of rifampicin on the pharmacokinetics of imatinib mesylate (Gleevec, STI571) in healthy subjects. *Cancer Chemother Pharmacol*. 2004;53:102-106. doi:10.1007/s00280-003-0722-9
20. Bowlin SJ, Xia F, Wang W, Robinson KD, Stanek EJ. Twelve-month frequency of drug-metabolizing enzyme and transporter-based drug-drug interaction potential in patients receiving oral

enzyme-targeted kinase inhibitor antineoplastic agents. *Mayo Clin Proc*. 2013;88:139-148. doi:10.1016/j.mayocp.2012.10.020

21. Grimstein M, Yang Y, Zhang X, et al. Physiologically based pharmacokinetic modeling in regulatory science: an update from the U.S. Food and Drug Administration's Office of Clinical Pharmacology. *J Pharm Sci*. 2019;108:21-25. doi:10.1016/j.xphs.2018.10.033
22. Gonzalez D, Rao GG, Bailey SC, et al. Precision dosing: public health need, proposed framework, and anticipated impact. *Clin Transl Sci*. 2017;10:443-454. doi:10.1111/cts.12490
23. Adiwidjaja J, Gross AS, Boddy AV, McLachlan AJ. Physiologically-based pharmacokinetic model predictions of inter-ethnic differences in imatinib pharmacokinetics and dosing regimens. *Br J Clin Pharmacol*. 2022;88:1735-1750. doi:10.1111/bcp.15084
24. Adiwidjaja J, Boddy AV, McLachlan AJ. Implementation of a physiologically based pharmacokinetic modeling approach to guide optimal dosing regimens for imatinib and potential drug interactions in paediatrics. *Front Pharmacol*. 2020;10:1672. doi:10.3389/fphar.2019.01672
25. Gao D, Wang G, Wu H, Wu JH, Zhao X. Prediction for plasma trough concentration and optimal dosing of imatinib under multiple clinical situations using physiologically based pharmacokinetic modeling. *ACS Omega*. 2023;8:13741-13753. doi:10.1021/acsomega.2c07967
26. Wojtyniak J-G, Britz H, Selzer D, Schwab M, Lehr T. Data digitizing: accurate and precise data extraction for quantitative systems pharmacology and physiologically-based pharmacokinetic modeling. *CPT Pharmacometrics Syst Pharmacol*. 2020;9:322-331. doi:10.1002/psp4.12511
27. Wojtyniak J-G, Selzer D, Schwab M, Lehr T. Physiologically based precision dosing approach for drug-drug-gene interactions: a simvastatin network analysis. *Clin Pharmacol Ther*. 2021;109:201-211. doi:10.1002/cpt.2111
28. Rüdesheim S, Wojtyniak JG, Selzer D, et al. Physiologically based pharmacokinetic modeling of metoprolol enantiomers and α-hydroxymetoprolol to describe CYP2D6 drug-gene interactions. *Pharmaceutics*. 2020;12:1200. doi:10.3390/pharmaceutics12121200
29. Marok FZ, Wojtyniak JG, Fuhr LM, et al. A physiologically based pharmacokinetic model of ketoconazole and its metabolites as drug–drug interaction perpetrators. *Pharmaceutics*. 2023;12:679. doi:10.3390/pharmaceutics15020679
30. Hanke N, Frechen S, Moj D, et al. PBPK models for CYP3A4 and P-gp DDI prediction: a modeling network of rifampicin, itraconazole, clarithromycin, midazolam, alfentanil, and digoxin. *CPT Pharmacometrics Syst Pharmacol*. 2018;7:647-659. doi:10.1002/psp4.12343
31. Türk D, Hanke N, Wolf S, et al. Physiologically based pharmacokinetic models for prediction of complex CYP2C8 and OATP1B1 (SLCO1B1) drug–drug–gene interactions: a modeling network of gemfibrozil, repaglinide, pioglitazone, rifampicin, clarithromycin and itraconazole. *Clin Pharmacokinet*. 2019;58:1595-1607. doi:10.1007/s40262-019-00777-x
32. Open Systems Pharmacology Suite Community. Open Systems Pharmacology Suite Manual, Version 11 2023. Accessed September 30, 2023. https://docs.open-systems-pharmacology.org/copyright
33. Guest EJ, Aarons L, Houston JB, Rostami-Hodjegan A, Galetin A. Critique of the two-fold measure of prediction success for ratios: application for the assessment of drug-drug interactions. *Drug Metab Dispos*. 2011;39:170-173. doi:10.1124/dmd.110.036103
34. Hegedus T, Orfi L, Seprodi A, Váradi A, Sarkadi B, Kéri G. Interaction of tyrosine kinase inhibitors with the human multidrug transporter proteins, MDR1 and MRP1. *Biochim Biophys Acta*. 2002;1587:318-325. doi:10.1016/S0925-4439(02)00095-9
35. D'Cunha R, Bae S, Murry DJ, An G. TKI combination therapy: strategy to enhance dasatinib uptake by inhibiting Pgp- and BCRP-mediated efflux. *Biopharm Drug Dispos*. 2016;37:397-408. doi:10.1002/bdd.2022
36. Langenbucher F. Linearization of dissolution rate by the Weibull distribution. *J Pharm Pharmacol*. 1972;24:979-981. doi:10.1111/j.2042-7158.1972.tb08930.x
37. Zidan DW, Hassan WS, Elmasry MS, Shalaby AA. A novel spectrofluorimetric method for determination of imatinib in pure, pharmaceutical preparation, human plasma, and human urine. *Luminescence*. 2018;33:232-242. doi:10.1002/bio.3406
38. Filppula AM, Tornio A, Niemi M, Neuvonen PJ, Backman JT. Gemfibrozil impairs imatinib absorption and inhibits the CYP2C8-mediated formation of its main metabolite. *Clin Pharmacol Ther*. 2013;94:383-393. doi:10.1038/clpt.2013.92
39. Jørgensen HG, Elliott MA, Allan EK, Carr CE, Holyoake TL, Smith KD. α1-acid glycoprotein expressed in the plasma of chronic myeloid leukemia patients does not mediate significant in vitro resistance to STI571. *Blood*. 2002;99:713-715. doi:10.1182/blood.V99.2.713
40. Peng B, Lloyd P, Schran H. Clinical pharmacokinetics of imatinib. *Clin Pharmacokinet*. 2005;44:879-894. doi:10.2165/00003088-200544090-00001
41. Friedecký D, Mičová K, Faber E, Hrdá M, Široká J, Adam T. Detailed study of imatinib metabolization using high-resolution mass spectrometry. *J Chromatogr A*. 2015;1409:173-181. doi:10.1016/j.chroma.2015.07.033
42. Rodríguez Flores J, Berzas JJ, Castañeda G, Rodríguez N. Direct and fast capillary zone electrophoretic method for the determination of Gleevec and its main metabolite in human urine. *J Chromatogr B Anal Technol Biomed Life Sci*. 2003;794:381-388. doi:10.1016/S1570-0232(03)00518-X
43. Eechoute K, Franke RM, Loos WJ, et al. Environmental and genetic factors affecting transport of imatinib by OATP1A2. *Clin Pharmacol Ther*. 2011;89:816-820. doi:10.1038/clpt.2011.42
44. Silva CG, Honeywell RJ, Dekker H, Peters GJ. Physicochemical properties of novel protein kinase inhibitors in relation to their substrate specificity for drug transporters. *Expert Opin Drug Metab Toxicol*. 2015;11:703-717. doi:10.1517/17425255.2015.1006626
45. van Erp NP, Gelderblom H, Karlsson MO, et al. Influence of CYP3A4 inhibition on the steady-state pharmacokinetics of imatinib. *Clin Cancer Res*. 2007;13:7394-7400. doi:10.1158/1078-0432.CCR-07-0346
46. Liu J, Chen Z, Chen H, et al. Genetic polymorphisms contribute to the individual variations of imatinib mesylate plasma levels and adverse reactions in Chinese GIST patients. *Int J Mol Sci*. 2017;18:603. doi:10.3390/ijms18030603
47. Frye RF, Fitzgerald SM, Lagattuta TF, Hruska MW, Egorin MJ. Effect of St John's wort on imatinib mesylate pharmacokinetics. *Clin Pharmacol Ther*. 2004;76:323-329. doi:10.1016/j.clpt.2004.06.007

48. Peng B, Hayes M, Resta D, et al. Pharmacokinetics and pharmacodynamics of imatinib in a phase I trial with chronic myeloid leukemia patients. *J Clin Oncol*. 2004;22:935-942. doi:10.1200/JCO.2004.03.050
49. Yang JS, Cho EG, Huh W, Ko JW, Jung JA, Lee SY. Rapid determination of imatinib in human plasma by liquid chromatography-tandem mass spectrometry: application to a pharmacokinetic study. *Bull Korean Chem Soc*. 2013;34:2425-2430. doi:10.5012/bkcs.2013.34.8.2425
50. Zhang Y, Qiang S, Yu Z, et al. LC-MS-MS determination of imatinib and N-desmethyl imatinib in human plasma. *J Chromatogr Sci*. 2014;52:344-350. doi:10.1093/chromsci/bmt037
51. Nikolova Z, Peng B, Hubert M, et al. Bioequivalence, safety, and tolerability of imatinib tablets compared with capsules. *Cancer Chemother Pharmacol*. 2004;53:433-438. doi:10.1007/s00280-003-0756-z

SUPPORTING INFORMATION

Additional supporting information can be found online in the Supporting Information section at the end of this article.

How to cite this article: Loer HLH, Kovar C, Rüdesheim S, et al. Physiologically based pharmacokinetic modeling of imatinib and *N*-desmethyl imatinib for drug–drug interaction predictions. *CPT Pharmacometrics Syst Pharmacol*. 2024;13:926-940. doi:10.1002/psp4.13127